Drosophila COP9 signalosome subunit 7 interacts with multiple genomic loci to regulate development

Ruth Singer[1], Shimshi Atar[2], Osnat Atias[1], Efrat Oron[1], Daniel Segal[3], Joel A. Hirsch[4], Tamir Tuller[2], Amir Orian[5] and Daniel A. Chamovitz[1,*]

[1]Department of Molecular Biology and Ecology of Plants, [2]Department of Biomedical Engineering, [3]Department of Molecular Microbiology and Biotechnology, [4]Department of Biochemistry and Molecular Biology, Tel Aviv University, Ramat Aviv, Tel Aviv 69978, Israel and [5]Cancer and Vascular Biology Research Center, Faculty of Medicine, Technion-Israel Institute of Technology, Haifa, Israel

ABSTRACT

The COP9 signalosome protein complex has a central role in the regulation of development of multicellular organisms. While the function of this complex in ubiquitin-mediated protein degradation is well established, results over the past few years have hinted that the COP9 signalosome may function more broadly in the regulation of gene expression. Here, using DamID technology, we show that COP9 signalosome subunit 7 functionally associates with a large number of genomic loci in the *Drosophila* genome, and show that the expression of many genes within these loci is COP9 signalosome-dependent. This association is likely direct as we show CSN7 binds DNA *in vitro*. The genes targeted by CSN7 are preferentially enriched for transcriptionally active regions of the genome, and are involved in the regulation of distinct gene ontology groupings including imaginal disc development and cell-cycle control. In accord, loss of CSN7 function leads to cell-cycle delay and altered wing development. These results indicate that CSN7, and by extension the entire COP9 signalosome, functions directly in transcriptional control. While the COP9 signalosome protein complex has long been known to regulate protein degradation, here we expand the role of this complex by showing that subunit 7 binds DNA *in vitro* and functions directly *in vivo* in transcriptional control of developmentally important pathways that are relevant for human health.

INTRODUCTION

The COP9 signalosome (CSN) protein complex was originally described as a negative regulator of light-induced growth patterns in plants (1). Subsequently it was found to have a central role in the regulation of development of multicellular organisms (2–4). In higher eukaryotes, the complex contains eight subunits, termed CSN1, for the largest subunit, to CSN8 for the smallest. Six of the CSN subunits, CSN1, 2, 3, 4, 7 and 8, contain a motif termed PCI (Proteasome-CSN-Initiation factor 3). A number of studies have indicated that the PCI domains interact to stabilize and form the backbone of these multiprotein complexes (5–7). Some of the subunits, including CSN7 are detected also in forms independent of the CSN core-complex (8–10).

The most studied CSN function is regulation of protein degradation. The CSN regulates cullin-RING E3 ligase (CRL) activity by removal of the ubiquitin-like protein Nedd8, from the cullin subunit of CRLs. This deneddylation activity localizes to CSN5 and is dependent on the integrity of the complete CSN complex (11,12). However, CSN5-dependent deneddylation is apparently only one aspect of CSN function (5,9,13–16).

Many CSN activities impinge on transcriptional regulation. Through its regulation of protein degradation, the CSN affects the stability of transcription factors (17–19). Yet, several studies hint that the nuclear CSN regulates transcription directly. For example, CSN2 (Alien) interacts with the corepressor SIN3 (20,21), and several studies revealed an association of CSN subunits to specific genes (22–24). These results together lead to the hypothesis that the CSN functions more broadly in the regulation of gene expression (25).

This hypothesis was backed up by structural studies showing that CSN7 has characteristics of known nucleic acid-binding proteins (26,27). The PCI domain contains a putative nucleic acid-binding motif in its winged-helix subdomain, which is comprised of a canonical helix-turn-helix.

Here we show that *Drosophila* CSN7 indeed binds DNA and functionally associates with a large number of loci in the *Drosophila* genome. Furthermore, we show that the transcription of many of these genes *in vivo* is dependent on

---

the entire CSN complex. Disruption of CSN7 leads to cellular and developmental phenotypes, which correlate with the predicted functions of CSN7 targets. Our results open a new line of studies for understanding how the CSN functions as a transcriptional regulator of developmentally-regulated genes and has direct implications for CSN involvement in human disease.

MATERIALS AND METHODS

'Fly growth conditions' were as published (9) with the following additions: Canton-S (CS) strain was used as wild type. RNAi-csn7 (#40691), RNAi-csn8 (#50565) and RNAi-*csn2* (#48044) were obtained from VDRC stock center. Csn7^p (#18023), *Actin*-GAL4 (#3954) and *Engrailed*-GAL4 (#25752) were obtained from Bloomington stock center. Additional information including complementation analysis and transgenic flies is found in the Supplementary Methods.

Cell lines and cell culture

Drosophila Kc167, SR$^+$ and S2 cell lines were cultured in SFX medium (Thermo Scientific HyClone) supplemented with L-glutamine, and Schneider media supplemented with 10% fetal bovine serum (FBS) (Biological Industries) and penicillin–streptomycin (Biological Industries), respectively, at 25°C. The RNAi procedures are detailed in the Supplementary Methods.

Anisotropy experiments

Expression and purification of CSN7 was as described (26). For binding assays, the DNA strands were synthesized and labeled using fluorescein attached through a six-carbon linker to the 5' end of the oligonucleotide primer used for polymerase chain reaction (PCR) synthesis. CSN7 protein was serially diluted from 4000 to 25 nM in buffer solution consisted of 10 mM Tris–HCl, 1 mM EDTA, 0.1 mM dithiothreitol (DTT) and 75 mM KCl, to a final volume of 60 μl. The indicated DNA was added to a final concentration of 3 nM and in competition experiments to final concentration of 150 nM. The anisotropy was measured using Horiba Jobin Yvon FL3-11 spectrofluorometer at 16°C. The titration was repeated twice. Titration curves were fit to a standard four-parameter binding curve using Sigmaplot (Systat). The equation used was:

$$\Delta r = \min + \frac{\max - \min}{1 + \left(\frac{[\text{CSN7}]}{\text{EC50}}\right)^{-\text{Hill slops}}}$$

where *r* is anisotropy, max and min are the respective maximal and minimal anisotropy values and the EC50 we treat as the $K_{\text{D app}}$.

'DamID' was carried out in Kc167 cells as described (28). The pNDamMyc-CSN7 fusion construct is described in Supplementary Methods. Samples were hybridized to a custom NimbleGen Drosophila 385k array (29).

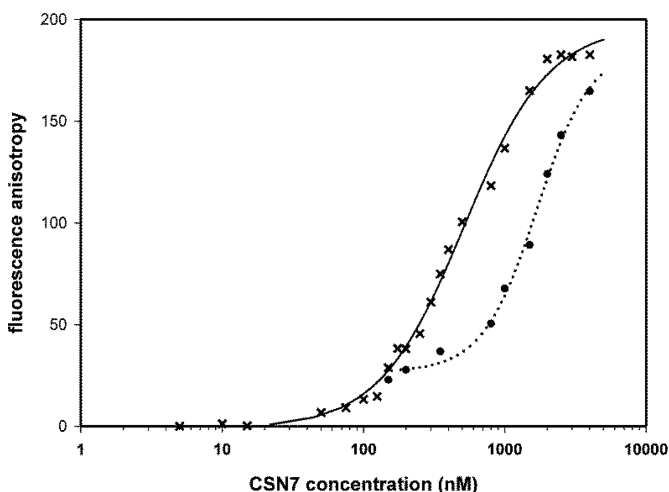'Immunohistochemistry' techniques are described in the Supplementary Methods. Primary antibody used: αCSN7

Figure 1. CSN7 interacts with DNA. Anisotropy binding profile for binding of full-length CSN7 to 3-nM fluorescein-labeled oligonucleotide derived from the *Drosophila E2f* promoter at 16°C (x). A 50-fold excess of unlabeled *E2f* oligonucleotide (·) at [150 nM] was added to 3 nM of fluorescein-labeled oligonucleotide as a competitor and titrated by CSN7. The $K_{\text{D app}}$ of CSN7 for this DNA fragment is 0.51 ± 0.03 μM with a Hill slope of 1.45, whereas the curve with unlabeled DNA had a $K_{\text{D app}}$ constant of 1.7 ± 0.16 μM with a Hill slope of 2.3. Due to the likelihood of multiple binding sites, caution should be exercised in overinterpreting these parameters as they represent an empirical characterization of the binding rather than providing a rigorous binding model.

(2); secondary antibody: FITC-conjugated Goat α Rabbit, Hoechst3342, Phalloidin (Sigma).

'Quantitative real-time PCR' was as described (14).

Flow cytometry

Third instar larvae were dissected in phosphate buffered saline (PBS) and about 30–50 imaginal wing discs were dissociated in 500 μl Trypsin-EDTA x10 (Sigma), 1 μl Vybrant DyeCycle orange 5 mM (Invitrogen) in PBS for 2–4 h at room temperature. SR$^+$ cells were grown for 4 days following RNAi treatment. Cells were harvested and precipitated on ice for 1 h followed by incubation with 1 μl Vybrant Dyecycle orange 5 mM (Invitrogen) for 30 min at room temperature. Fluorescence-activated cell sorting (FACS) analysis for cell-cycle profile was performed using the Becton Dickinson FACSort and CellQuest software.

'Chromatin immunoprecipitation (ChIP)' was modified from (30) and detailed in the Supplementary Methods. ChIP was performed using αCSN7 (2), αHistone-3 (Abcam, ab8580) or normal goat serum (NGS).

Computational analyses

For mapping to the genome and orthologs mapping, data were downloaded from Biomart (http://www.biomart.org/).

Data normalization. The *Csn7* DamID data analyses were based on quintile normalization of the four samples and average of the results.

P-*values and graphs.* The genomic positions of *Drosophila melanogaster* open reading frames were downloaded from
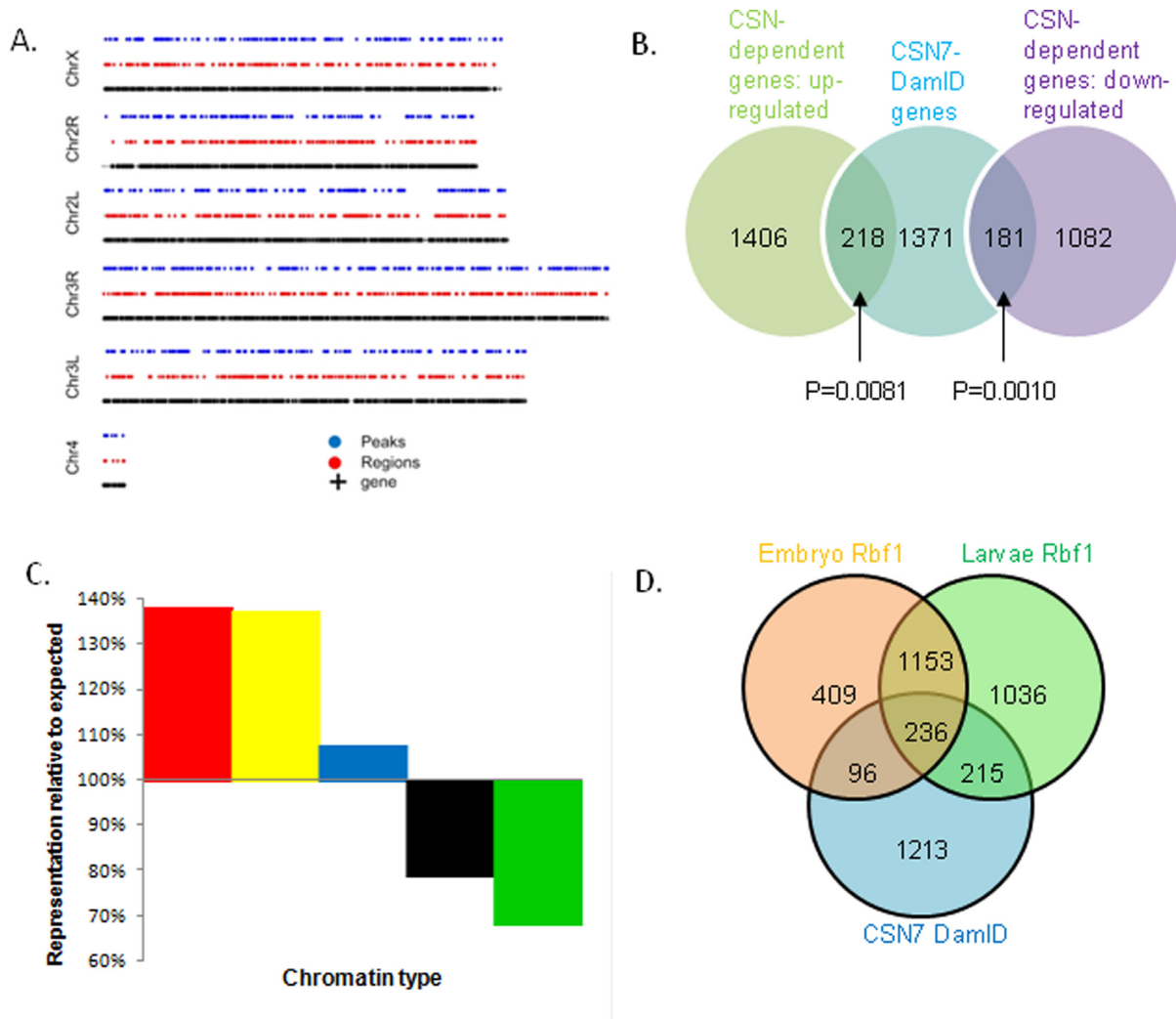
Figure 2. Analyses of the genes bound by CSN7 . (**A**) A global view on the DamID experiment. Black dots mark the positions of genes along the *D. melanogaster* genome; blue dots denote the positions of the most significant (top 10%) DamID signals; and red dots denote regions enriched in DamID signals, considering sliding windows of 1000 bp in length, and the top 49% of the scores. Dots are spaced minimally by 1000 bp. (**B**) CSN-dependent genes are preferentially enriched in the CSN7-DamID genes. Genes over- and underexpressed in *csn* mutants are significantly enriched in the CSN7-DamID results. Ten genes were both up- and downregulated, dependent on the mutant and stage; thus, the total number of genes in the graph (1770) is slightly larger than the actual total number of genes (1760). The *P*-values are based on hypergeometric distribution (which is based on the total number of genes, the number of gene in each set and the number of overlapping genes between the two sets). (**C**) Analyses of CSN7 enrichment in five chromatin types defined by Filion *et al.* (29) revealed a high overlap with 'red' and 'yellow' chromatin, while 'black' and 'green' chromatin were under-represented in the CSN7-DamID targets. 'Blue' chromatin was not affected by the CSN7-DamID. (**D**) Genes bound by CSN7 are significantly enriched in Rbf1 targets (*P*-value for overlap with CSN-DamID: Embryo = $7.3255e^{-11}$, Larvae = $4.2188e^{-15}$).

National Center for Biotechnology Information (NCBI). We employed two definitions related to the genes associated with the DamID peaks: these were defined as either (i) the 500 nt before and after the beginning of the ORF; or (ii) as genes mapped closest to the DamID peak (a definition that is used in all other analyses performed in the study).

For Figure 2A, genes were divided into groups according to their fold change in the *csn4null* mutant at time 60 h AED (4). For each group the mean signal based on the CSN7 DamID experiment over the genomic region defined above was computed.

In the case of definition 1, the *P*-value *k*-test when comparing the DamID experiment of the overexpressed genes to the ones that do not change significantly and when comparing the DamID experiment of the underexpressed genes to the ones that do not change significantly are ($P = 0.00977$; KS-test) for significant increase in fold change versus no significant change in fold change and ($P = 0.0113$; KS-test) for significant decrease in fold change versus no significant change in fold change and respectively. The difference in DamID signals between genes with significant increase in fold change and gene with significant decrease in fold change is not significant ($P = 0.067$ KS-test).

Enrichment *P*-value related to CNS7-DamID and differentially expressed genes (definition 2) in *csn* mutant experiments (Figure 2C) was computed based on hypergeometric *P*-value ($P = 5.5*e-05$).

To compute the enrichment of genes regulated by CSN7 among orthologs of human disease genes, a list of 6548 human disease genes was downloaded from gene-card database 2013 (http://www.genecards.org/) (31). The enrichment *P*-value was computed based on hypergeometric distribution considering the following numbers: the number of human genes with *Drosophila* orthologs (5801 genes); the number of human disease genes with fly orthologs (2165 genes); the number of human genes (with fly orthologs) that are orthologous to DamID significant genes in fly (1014 genes); the number of human genes that (i) are disease genes, (ii) have *Drosophila* orthologs, (iii) their fly orthologs are DamID significant (410 genes).

To identify transcription factor (TF)-binding sites, we used the genome versions BDGP R5/dm3 and BDGP R4/dm2 of *Drosophila* (Apr. 2006 [BDGP R5/dm3] for the DamID experiment; Apr. 2004 [BDGP R4/dm2]—for the TFs), downloaded from the UCSC genome browser (http://genome.ucsc.edu/). Binding site positions of various TFs were downloaded from mod-ENCODE (www.modencode.org). We considered two TFs binding site datasets 'Fly Transcription Factors by chIP-chip' (http://intermine.modencode.org/release-32/ template.do?name = TF_BindingSites&scope = all) and 'REDfly *Drosophila* transcription factor binding sites' (http://www.flymine.org/release-37.1/template.do?name = Dataset_TF_BindingSites&scope = all). For each transcript start site, we considered the region of up to 2000 nt upstream and 2000 nt downstream, though the results are robust to small changes in these definitions. We computed for each TF a hypergeometric *P*-value considering the enrichment of the TF-binding sites in the same genes with CSN7-DamID-binding sites; to this end, we considered the total number of genes that include binding sites of the TF, the total number of genes that include binding sites of the CSN7-DamID, the total number of genes and the total number of genes that include binding sites of the CSN7-DamID and also binding sites of the TF. The *P*-values were filtered based to control for a false discovery rate of 5%.

'To identify sequence motifs enriched in the CSN7-binding sites', we employed the HOMER (Hyper-geometric Optimization of Motif Enrichment) tool (32). To this end, we compared the set CSN7-binding sites after adding 50 nt to both end of the sites to a background set composed in the following way: for each CSN7-binding site of length *l,* we added to the background set two sequences of length *l* corresponding to the DNA regions 100 nt upstream and downstream to the binding site (as defined above); similar results were obtained for sites of distance 300 nt upstream and downstream to the binding site.

RESULTS

CSN7 binds DNA directly

As earlier biophysical and cell biology studies suggested that CSN7, or the CSN in general, binds nucleic acids (25), we carried out binding assays (33) to study the potential interaction of purified full-length CSN7 protein with a fluorescently-labeled DNA fragment, 70 bp in length. Steady-state fluorescence anisotropy of fluorescein-labeled

DNA, derived from *E2f*, was monitored upon titration with the full-length CSN7 protein. Figure 1 (x) shows a representative binding isotherm. The anisotropy increases in a saturable manner, demonstrating binding of CSN7 to this DNA fragment. The anisotropy values suggest that multiple protein copies bind this fragment.

To examine binding specificity, the binding of CSN7 to the labeled DNA fragment was challenged with 50-fold excess of unlabeled DNA. As observed in Figure 1 (circles), this excess of unlabeled DNA fragment induced a marked shift in the titration curve indicating that the unlabeled DNA competitively binds CSN7 protein. Fitting of the binding data indicates that CSN7 interacts with this fragment with an apparent K_D of about 500 nM. This value is within the range of non-sequence-specific DNA-binding proteins (34). We have chosen to present a $K_{D\ app}$ constant since determination of bona fide affinity constants will require delimitation of a target DNA site and subsequent binding isotherms with these defined sites. Similar studies were carried out with a different labeled DNA fragment, derived from the *CycE* open reading frame, yielding similar anisotropy profiles (Supplementary Figure S1), while experiments using the maltose-binding protein yielded no increase in anisotropy providing a negative control.

While CSN7, like five other CSN subunits, contains a PCI domain, which harbors a putative nucleic acid-binding motif (21,22), this winged-helix subdomain on its own is not stable (21), so we could not further test if this domain alone is involved in nucleic acid binding.

Drosophila CSN7 associates with multiple genomic loci

The binding of CSN7 to DNA detected above, together with the earlier studies where other CSN subunits were detected in association with several specific genes (22–24), led us to hypothesize that CSN7 interacts with multiple regions in the *Drosophila* genome. Thus, as a starting point to identify the genomic regions bound by CSN7, we performed DamID chromatin profiling in *Drosophila* Kc167 cells (28,29). We determined that CSN7 binds to ∼9400 regions genome-wide and overlaps with gene-rich regions (Figure 2A), corresponding to ∼1700 genes (Dataset S1). CSN7 binding was detected preferentially in promoter, exon and intron regions, while excluded from both the 5′ and 3′ UTR regions, and in regions defined as intergenic (Table 1, Supplementary Table S1). These data have been uploaded to the UCSC Genome Browser for visual integration with other datasets. Supplementary Figure S2A and B show screenshots from the browser at the resolution of chromosome 3, and the region of the *e2f* gene, which is further analyzed below.

CSN-dependent genes are enriched for CSN7 targets

To connect between the genomic loci bound by CSN7 and active gene regulation, we compared our DamID data to our previous transcriptome analyses that suggested a direct role for the CSN in transcriptional control (14), and with additional transcriptomic data generated in our lab. Specifically we determined whether CSN7 associates with the genes misregulated in mutants in CSN subunits [*csn4^{null}*, *csn5^{null}, csn5^3; csn3^{null}, csn1$^{30.2}$*], and examined the CSN7

Table 1. The CSN7-DamID signal is enriched in genic regions

Region	Enrichment ratio	$P_{enrichment}$
Promoter	1.4694	$<10^{-30}$
Intron	1.1677	$<10^{-30}$
Exon	1.0955	$<10^{-30}$
Exon123	1.0747	$<10^{-30}$
5′-UTR	0.0038	1
3′-UTR	0.0003	1
Non-gene	0.9009	1

Analysis of the intersection of the CSN7-DamID signal with various genic regions. Enrichment ratio is based on data presented in Supplementary Table S1. The enrichment ratio is the fraction of the genic region containing the CSN7-DamID signal relative to the amount of the CSN7-DamID signal predicted for that gene if normal distribution. A value > 1 corresponds to higher overlap between the genic region and the CSN7-DamID signal than expected, with the corresponding enrichment *P*-value.

Table 2. Transcription regulators with binding sites enriched in the CSN7-DamID results

Transcriptional regulators	Total # genes with binding sites	# CSN7-DamID genes with binding sites	*P*-value
bric a brac 1	1358	148	6.29E-12
CTCF	7812	663	0
C-terminal Binding Protein	3183	252	1.32E-05
Dichaete	3020	297	0
Disconnected	2018	214	5.55E-16
GATAe	2361	201	1.30E-06
gooseberry-neuro	820	96	1.29E-09
Hairy	2851	257	7.19E-11
Huckebein	3268	267	4.53E-07
Jumeau	3069	267	1.12E-09
Nejire	9635	797	0
Trithorax-like	7193	640	0
Ultrabithorax	2863	281	1.11E-16
Zn finger homeodomain 1	755	91	8.24E-10

The list of transcription regulators with the lowest *P*-values for enrichment in the CSN7-DamID results.

DamID-signal distribution for these genes relative to genes whose expression is not altered in these mutants.

We used two different statistical approaches in this analysis. In the first, we looked at the average DamID signal at the beginning of the open reading frame of all the CSN-dependent genes, relative to genes whose expression is not affected by the *csn* mutants. In the second, we compared DamID signals in different groups of genes, looking for significant enrichment in the CSN-dependent genes differentiated by up- or downregulation (see Supplementary Methods). Using both approaches, the CSN-dependent genes were preferentially enriched in the CSN7-DamID genes. For the first approach, the overlap of 389 genes was found to be significant ($P = 5.5*e^{-5}$). As seen in Figure 2B, the second approach also identified a significant overlap between the DamID and CSN-dependent genes. We found enrichment between the CSN-dependent and the CSN7-DamID genes only when considering all mutants together and not for a mutant in a particular subunit. This is likely due to the reduced statistical power of smaller groups comparisons to all genes. Nevertheless, groups of genes in all mutants were represented in the CSN7-DamID results (Supplementary Table S2).

Since CSN4 and CSN3 are essential for the integrity of the entire CSN complex (9), our finding that CSN7 preferentially binds to CSN-regulated genes strongly suggests an interaction of the CSN holo-complex with these loci.

CSN7 targets genes involved in central developmental processes

Filion *et al.* (29) identified five distinct chromatin types in *Drosophila* by DamID profiling of 53 different proteins. These chromatin types were arbitrarily given the colors red, yellow, black, blue and green where 'red' and 'yellow' chromatin are defined as transcriptionally active and are similar to the classic definition of euchromatin, and 'green' and 'black' chromatin are defined as heterochromatic or repressed chromatin. We analyzed these chromatin states for enrichment of CSN7 binding and found a high overlap with 'red' and 'yellow' chromatin, while 'black' and 'green' chromatin were under-represented in the CSN7-DamID targets. These over- and under-representations of CSN7-DamID targets were significant compared to other chromatin states, as well as a control cohort randomized version of the genome (Figure 2C). Thus, CSN7 in Kc167 cells preferentially targets transcriptionally active regions of the *Drosophila* genome.

We further tested if the CSN7-DamID targets are enriched for binding sites of known transcription regulators (TR). Binding site positions of various TRs were based on the ChIP-chip data from modENCODE (35). We considered the region of up to 2000 nt upstream and 2000 nt downstream to the start site of each transcript, and mined for an overlap between TR-binding sites and the CSN7-DamID signal. We computed for each TR a hypergeometric *P*-value considering the enrichment of the TR-binding sites in the

Table 3. Signaling pathways enriched in CSN7-DamID genes

	Ontology grouping	Genes present in CSN7-DamID	*P*-value
Functional GO clusters	Imaginal disc development	104	3.50E-10
	Cytoskeleton organization	109	1.10E-08
	Cell morphogenesis	102	8.40E-08
	Regulation of transcription	148	8.20E-05
	Ion binding	304	8.40E-04
	Chromatin organization	47	3.20E-06
	Gamete generation	138	2.00E-08
	Nucleotide binding	227	1.70E-05
	Cell cycle	111	2.00E-03
	Cell motion	72	3.80E-06
	Regulation of cell development	46	1.70E-09
	Tissue morphogenesis	60	1.10E-05
	ATP binding	113	1.30E-04
KEGG pathways	Dorso-ventral axis formation	29	2.21E-07
	PDGF signaling pathway	27	3.06E-06
	Jak-STAT signaling pathway	22	4.09E-06
	Gonadotropin releasing hormone receptor pathway	28	5.42E-05
	Integrin signaling pathway	28	9.43E-05
	Interleukin signaling pathway	18	2.86E-04
	PI3 kinase pathway	19	4.65E-04
	EGF receptor signaling pathway	24	1.04E-03
	Insulin/IGF pathway-mitogen activated protein kinase kinase/MAP kinase cascade	11	1.23E-03
	Progesterone-mediated oocyte maturation	25	1.27E-03
	Notch signaling pathway	16	2.50E-03
	FGF signaling pathway	22	3.43E-03
	Wnt signaling pathway	36	3.60E-03
	Ras pathway	14	1.55E-02
	MAPK signaling	13	1.80E-02
	Ubiquitin-mediated proteolysis	39	1.80E-02
	Endothelin signaling pathway	21	1.97E-02
	FAS signaling pathway	9	2.22E-02
	Circadian rhythm	9	3.03E-02
	Hedgehog signaling pathway	11	3.66E-02

Ontology groupings were found using the David Bioinformatics Database, Panther or Babelomics servers.

same genes with CSN7-DamID-binding sites. The *P*-values were filtered to a false discovery rate of 5% (36).

The CSN7-DamID targets are significantly enriched for binding of at least one of 23 distinct TRs with central roles in *Drosophila* development (Table 2). These include both sequence-specific transcription factors such as CTCF (37), and transcriptional corepressors/activators like CtBP (38).

Ullah *et al.* (2007) showed that CSN4 associates with the Retinoblastoma family protein Rbf1 on specific promoters in both *Drosophila* S2 cells and in embryos. Recently it has been shown using chromatin IP technology that Rbf1 associates with multiple target genes involved in diverse signaling pathways (39,40). This led us to ask if there is an overlap between the CSN7 and the Rbf1-binding profiles. As seen in Figure 2D, there is a significant overlap between the CSN7 DamID targets in Kc167 cells and the Rbf1 ChiP targets in both embryo and larvae (Dataset 3). This overlap was identified for targets that were detected with complementary approaches (DamId for CSN7 versus ChIP for Rbf1) and using different starting material (Kc167 cells for CSN7 versus embryos and larva for Rbf1), emphasizes the robustness of the overlap.

In an attempt to discover if CSN7 associates with specific nucleic acid sequences, we searched for enriched sequence motifs using a computational tool for finding consensus sequence motifs (HOMER (32)). To this end, we compared the set of CSN7-DamID sites to background sequences at a distance of 100 (x) nt from the CSN7-DamID sites and with identical size (more details in the Supplementary Methods). Following a few iterations of this approach with different x (100, 300) we did not succeed in finding a sequence motif that appears in the CSN7-DamID sites but not in the background sequences; all the motifs enriched in the CSN7-DamID sites also appeared in at least 42% of the background sequences. While a negative result, from this we conclude that the overall binding of CSN7 to the chromatin does not appear to be sequence specific.

The CSN7-DamID targets were further analyzed for enrichment of Gene Ontology (GO) terms. One hundred sixty GO terms were found to be significantly enriched in the CSN7-DamID targets (Dataset S2). To distill this data, we employed the 'Functional Annotation' tool of the DAVID Bioinformatics Database (41), which revealed that CSN7 associates preferentially with genes involved in central developmental and related pathways, including those involved
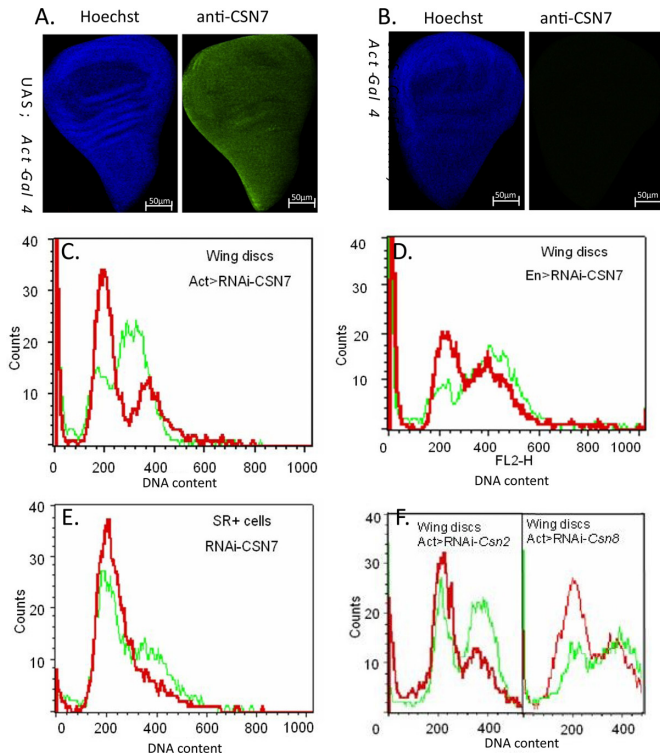
Figure 3. (**A** and **B**) Silencing *Csn7* affects patterning of the wing imaginal disc. Silencing *Csn7* (B) results in changes of the wing disc compared to control (A). The folds in the wing disc are clearly seen in the confocal image of the control disc stained with α-CSN7 or Hoechst, but not when CSN7 is silenced. CSN7 is not detected in (A). (**C** and **D**) Cell-cycle profiles of cells dissociated from wing discs expressing the UAS-RNAi-CSN7 construct under the control of the *Act-* (C) or *En-* (D) Gal4 (red) relative to profiles of dissociated cells from wing discs expressing the *Act* or *En-*Gal4 drivers alone (green). (**E**) Cell-cycle profile of SR⁺ cells silenced for CSN7 using CSN7-RNAi (red) relative to control cells (green). (**F**) Cell-cycle profiles of cells from dissociated wing discs expressing the *Act>RNAi-Csn2* and *Act>RNAi-Csn8*.

in imaginal disc development, cell-cycle, transcriptional regulation and oogenesis (Table 3). Key signaling pathways are also enriched in the CSN7-DamID results (Table 3). The group of genes bound by both CSN7 and Rbf1 are also specifically enriched for genes involved processes such as cell-cycle, oogenesis and wing disc development (Dataset 3).

We also asked if the *Drosophila* CSN7-DamID targets tend to have human orthologs in disease genes. Of 2165 human disease genes with clear *Drosophila* homologues (37), 547 of these were identified in the CSN-DamID results (Dataset S4), which is a significant enrichment beyond expected for a random distribution (*P*-value = 0.0134). These include a wide range of disease types including various cancer (e.g. breast or pancreatic cancer), neurologic (e.g. two different genes implicated in Alzheimer's disease, nine in mental retardation, three in Parkinson disease) and metabolic disorders (e.g. one gene implicated in congenital disorders of glycosylation, and five genes involved in diabetes).

CSN7 is essential for wing disc development and G1-S cell-cycle progression

To experimentally test these bioinformatic predictions, we examined whether loss of CSN7 function impacts these biological processes and affects expression of the target genes through analyses of *Drosophila* carrying a null mutation in *Csn7*. Bloomington stock center strain (#18203, termed here *csn7ᵖ*) has a P-element insertion in the second intron of the *Csn7* gene and when homozygous results in a complete loss of *Csn7* transcript and protein (Supplementary Figure S2); thus, *csn7ᵖ* should be considered a null allele. Similar to mutations in other CSN subunits (14,42), *csn7ᵖ* is recessive lethal, with double mouth-hooks appearing after the second ecdysis concurrent with the primary lethal phase, and melanotic tumors developing during the third instar stage in surviving larvae, which then arrest 120 h after egg deposition (Supplementary Figure S3). These phenotypes are linked solely to the *Csn7* locus, as all phenotypes were complemented by the expression of a UAS-*Csn7-GFP* transgene driven by an *Act*-GAL4 driver (Supplementary Figure S4).

Furthermore, targeted reduction of *Csn7* expression via a *Csn7*-RNAi transgene under the control of the *Act*-Gal4 driver resulted in pupal lethality, which was preceded by the appearance of melanotic tumors (Supplementary Figure S3). As expected, expression of this transgene was effective in reducing both transcript and protein levels of CSN7.

Next, we examined the role of CSN7 in imaginal disc formation and cell-cycle progression, two of the GO groupings identified as enriched in CSN7-DamID targets. Imaginal wing discs in third instar *csn7ᵖ* larvae are severely reduced in size, which correlates with the enrichment of genes associated with imaginal discs identified by DamID. As the size of the imaginal wing discs from the *csn7 ᵖ* mutant discs precluded further analyses, we specifically targeted CSN7 using UAS-*Csn7*-RNAi transgene under either *Act*-Gal4 or *En*-Gal4. While these wing discs were of normal size, they were developmentally defective as the folds in the wing pouch and hinge were not readily evident (Figure 3A and B).

To garner additional information about the nature of this wing phenotype, we carried out flow cytometry (FACS) analysis on dissociated cells from wing discs expressing the *Csn7*-RNAi transgene under either *Act*-Gal4 or *En*-Gal4 control. Expression of the *Csn7*-RNAi transgene under either driver resulted in a cell-cycle profile consistent with a proliferation defect: the G1 fraction was increased at the expense of G2 relative to the wild type (Figure 3C–D). A similar G1 enrichment was obtained for *Drosophila* SR⁺ cells transfected with a CSN7-RNAi construct (Figure 3E), further indicating that CSN7 preferentially promotes G1/S progression. This cell-cycle phenotype is likely a result of loss-of-function of the entire CSN complex as RNAi-mediated downregulation of CSN2 or CSN8 resulted in similar G1 delays (Figure 3F).

Endogenous CSN7 associates with the regions identified by DamID

The bioinformatic analysis above clearly illustrated that CSN-dependent genes are enriched in the CSN7-DamID dataset. To further connect between the genes bound by CSN7 and the phenotypes described above, we determined
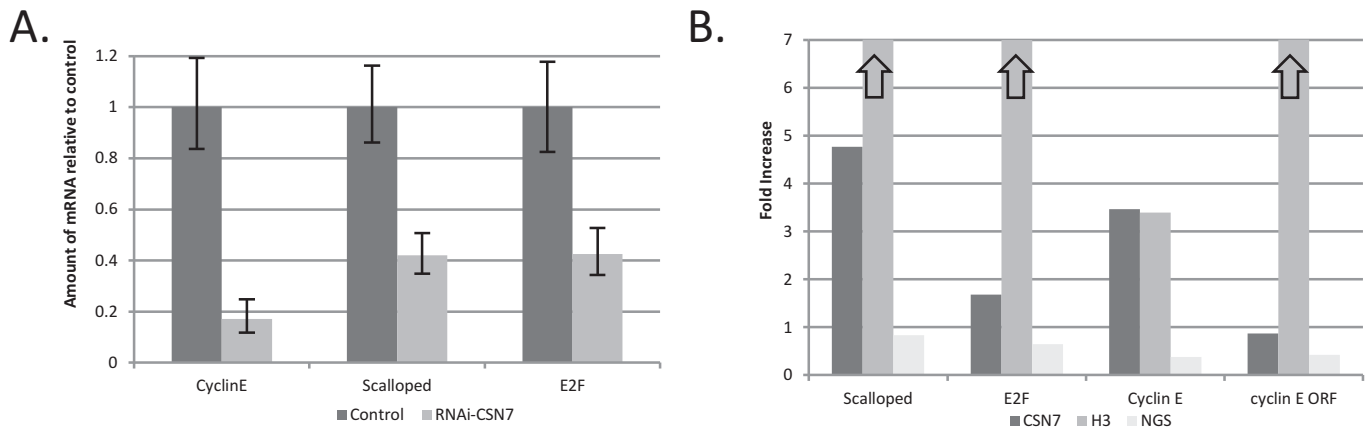
Figure 4. (**A**) qRT-PCR analyses of CSN7-DamID target genes in RNA isolated from Kc167 cells following transfection with an RNAi-CSN7 construct. The levels of *CycE, E2f* and *Scalloped* were downregulated relative to cells transfected with a control RNA. The columns show the geometric mean of the expression, with the error bars representing the minimal and maximal deviations. (**B**) ChIP. Chromatin was isolated from cross-linked Kc167 cells and subjected to immuno-precipitation (IP) with αCSN7, αH3 or NGS followed by qRT-PCR. PCR primers were designed around the predicted binding regions for CSN7 in the *Sd, E2F and CycE* genes (Supplementary Table S2), and around a region ~2.5 kb downstream from the predicted CSN7 target in *CycE*. The predicted binding regions of all three genes were precipitated with the positive control αH3, and with αCSN7, significantly beyond the signal for the negative control NGS. (*P*-values for significance above background: *Sd*, 9.72e-04; *E2F*, 0.01; *CycE*, 0.01). Moreover, while αH3 also precipitated the ORF of Cyclin E, αCSN7 did not, showing specificity for interaction with the promoter region only, as identified by the DamID experiment.

if the expression of the genes within the CSN7-DamID loci is also misregulated upon RNAi-mediated reduction of CSN7. We examined by qRT-PCR the mRNA levels of three key developmental genes involved in cell-cycle regulation and wing disc development, *CycE, E2f* and *Scalloped* (*Sd*). mRNA levels were checked in Kc167 and S2 cells where we reduced CSN7 levels via RNAi. As shown in Figure 4A and Supplementary Figure S6, the levels of *CycE and E2f* were reduced when *Csn7* was silenced in both cell types, while *Sd* was reduced only in Kc167 cells.

We further investigated if the genomic regions identified as bound by the CSN7-Dam fusion protein for these three genes (see Supplementary Figure S2 for specific example of *e2f*) are indeed occupied by endogenous CSN7 by performing ChIP with anti-CSN7 antibodies. Anti-histone H3 served as a positive control and NGS as a negative control. As seen in Figure 4B, the regions identified by DamID of all three genes mentioned above were bound with CSN7 and histone H3, but not control IP. While the IP signal above background for the three genes varied, possibly due to affinity issues, they were significant, ranging from 4.6 to 35.7 standard deviations (see legend of Figure 4B for *P*-values). The validity of the IP results *vis a vis* the DamID results is further supported by the negative control where anti-histone H3 precipitated a second region of *CycE*, 2.5 kb downstream of the DamID-predicted CSN7-occupied region, while anti-CSN7 did not.

DISCUSSION

We present here the first global genomic description of a CSN subunit binding to chromatin. While a number of earlier studies had indicated that certain CSN subunits associate with specific genes, it was unclear from these studies whether these results were indicative of a broader function of the CSN in regulating gene expression on the chromatin, or rather were isolated incidents (22–24). Using DamID

technology, we showed that *Drosophila* CSN7 associates with ~10% of *Drosophila* protein-encoding genes. Thus, the data presented here expand the arsenal of functions attributed to the CSN. Not only does CSN7 associate with chromatin, but it is associated with genomic regions known to be misregulated in the absence of the CSN. Thus, CSN7, and by extension the entire CSN, could now be considered a transcriptional regulator.

Defining the CSN as a transcriptional regulator echoes back 20 years to the original description of the *cop9* mutant in Arabidopsis. Wei and Deng (43) reported high-level expression of light-inducible genes in the absence of light in these mutants, and hypothesized that COP9 acts by altering the promoter activities of these genes. Later the CSN was found not only to be a signal-dependent repressor of transcription, but also a signal-dependent inducer of some of the same genes (44). While work in many labs established the paradigm of the CSN regulating gene expression through modulating the stability of transcription factors (17,18), the results presented here reopen the door for the CSN having a direct role in global transcriptional regulation on the chromatin. This role likely involves a direct interaction between the CSN and DNA, as clearly shown in the anisoptry studies with CSN7.

Importantly though, we do not propose that CSN7 is a sequence-specific DNA-binding protein, but rather functions as a co-regulator of transcription that is recruited to targets by specific factors. Indeed, CSN7 interacts *in vitro* with oligonucleotides derived from both regions predicted to bind CSN7 and regions not identified as binding CSN7, suggesting that the affinity is for DNA in general. This is also supported by the *in vitro* K_d, which is higher than that of sequence-specific DNA-binding proteins, but in line with other general binding proteins, and by our inability to identify enriched sequences in the CSN7-DamID sites. We propose that the specificity in CSN7 targeting is mediated through interacting proteins. Indeed, CSN subunits have

been conspicuous for their ability to fish-out key transcriptional regulators in protein–protein interaction studies (45–48). Thus while each interacting protein may have a specific target site, the presence of multiple target sites in our data precluded the possibility of detecting these through bioinformatic analysis.

Of course, these two roles proposed for the CSN, chromatin binding and regulation of TR stability, are not mutually exclusive. It is conceivable that the CSN regulates TR stability directly on the chromatin, similar to the activity of the proteasome on chromatin (49). Indeed many of the transcriptional regulators whose binding sites are enriched in the CSN7-DamID targets (Table 1) are either substrates of the proteasome [e.g. Hairy (50)] or components of the degradation machinery [e.g. bric—a-brac (51)], such that the function of the CSN on the chromatin may be intimately connected with its role in protein degradation.

Yet, other evidence does point to a proteasome-independent role for the CSN. Indeed an N-terminal fragment of human CSN1 translocates to the nucleus and inhibits gene expression from a number of specific promoters (10). Although the mechanism of this inhibition is still unclear, it might be related to the fact that this part of CSN1 interacts with SAP130—a member of the DDB1 protein family and an established component of the transcription machinery (20). This fits very well with other observations for ubiquitin-like modifications that regulate chromatin structure and gene activity independent of degradation (52).

Regardless of the mechanism, the results presented here have implications for the role of the CSN in human biology. Considering the number of key signaling pathways bound by CSN7, it is not surprising that so many human disease genes have homologs with significant binding signal of CSN7. Thus further elucidating the mechanism by which the CSN is recruited to different loci could have major implications for biomedical research.

SUPPLEMENTARY DATA

Supplementary Data are available at NAR Online.

ACKNOWLEDGMENTS

FUNDING

REFERENCES

1. Chamovitz,D.A., Wei,N., Osterlund,M.T., von Arnim,A.G., Staub,J.M., Matsui,M. and Deng,X.W. (1996) The COP9 complex, a novel multisubunit nuclear regulator involved in light control of a plant developmental switch. *Cell*, **86**, 115–121.
2. Freilich,S., Oron,E., Kapp,Y., Nevo-Caspi,Y., Orgad,S., Segal,D. and Chamovitz,D.A. (1999) The COP9 signalosome is essential for development of Drosophila melanogaster. *Curr. Biol.*, **9**, 1187–1190.
3. Wei,N., Tsuge,T., Serino,G., Dohmae,N., Takio,K., Matsui,M. and Deng,X.W. (1998) The COP9 complex is conserved between plants and mammals and is related to the 26S proteasome regulatory complex. *Curr. Biol.*, **8**, 919–922.
4. Seeger,M., Kraft,R., Ferrell,K., Bech-Otschir,D., Dumdey,R., Schade,R., Gordon,C., Naumann,M. and Dubiel,W. (1998) A novel protein complex involved in signal transduction possessing similarities to 26S proteasome subunits. *FASEB J.*, **12**, 469–478.
5. Enchev,R.I., Scott,D.C., da Fonseca,P.C., Schreiber,A., Monda,J.K., Schulman,B.A., Peter,M. and Morris,E.P. (2012) Structural basis for a reciprocal regulation between SCF and CSN. *Cell Rep.*, **2**, 616–627.
6. Sharon,M., Taverner,T., Ambroggio,X.I., Deshaies,R.J. and Robinson,C.V. (2006) Structural organization of the 19S proteasome lid: insights from MS of intact complexes. *PLoS Biol.*, **4**, e267.
7. Zhou,M., Sandercock,A.M., Fraser,C.S., Ridlova,G., Stephens,E., Schenauer,M.R., Yokoi-Fong,T., Barsky,D., Leary,J.A.,, Hershey,J.W. *et al.* (2008) Mass spectrometry reveals modularity and a complete subunit interaction map of the eukaryotic translation factor eIF3. *Proc. Natl Acad. Sci. U.S.A.*, **105**, 18139–18144.
8. Fukumoto,A., Tomoda,K., Kubota,M., Kato,J.Y. and Yoneda-Kato,N. (2005) Small Jab1-containing subcomplex is regulated in an anchorage- and cell cycle-dependent manner, which is abrogated by ras transformation. *FEBS Lett.*, **579**, 1047–1054.
9. Oron,E., Mannervik,M., Rencus,S., Harari-Steinberg,O., Neuman-Silberberg,S., Segal,D. and Chamovitz,D.A. (2002) COP9 signalosome subunits 4 and 5 regulate multiple pleiotropic pathways in Drosophila melanogaster. *Development*, **129**, 4399–4409.
10. Tsuge,T., Matsui,M. and Wei,N. (2001) The subunit 1 of the COP9 signalosome suppresses gene expression through its N-terminal domain and incorporates into the complex through the PCI domain. *J. Mol. Biol.*, **305**, 1–9.
11. Cope,G.A., Suh,G.S., Aravind,L., Schwarz,S.E., Zipursky,S.L., Koonin,E.V. and Deshaies,R.J. (2002) Role of predicted metalloprotease motif of Jab1/Csn5 in cleavage of Nedd8 from Cul1. *Science*, **298**, 608–611.
12. Enchev,R.I., Schreiber,A., Beuron,F. and Morris,E.P. (2010) Structural insights into the COP9 signalosome and its common architecture with the 26S proteasome lid and eIF3. *Structure*, **18**, 518–527.
13. Dohmann,E.M., Kuhnle,C. and Schwechheimer,C. (2005) Loss of the CONSTITUTIVE PHOTOMORPHOGENIC9 signalosome subunit 5 is sufficient to cause the cop/det/fus mutant phenotype in Arabidopsis. *Plant Cell*, **17**, 1967–1978.
14. Oron,E., Tuller,T., Li,L., Rozovsky,N., Yekutieli,D., Rencus-Lazar,S., Segal,D., Chor,B., Edgar,B.A. and Chamovitz,D.A. (2007) Genomic analysis of COP9 signalosome function in Drosophila melanogaster reveals a role in temporal regulation of gene expression. *Mol. Syst. Biol.*, **3**, 108.
15. Emberley,E.D., Mosadeghi,R. and Deshaies,R.J. (2012) Deconjugation of Nedd8 from Cul1 is directly regulated by Skp1-F-box and substrate, and the COP9 signalosome inhibits deneddylated SCF by a noncatalytic mechanism. *J. Biol. Chem.*, **287**, 29679–29689.
16. Fischer,E.S., Scrima,A., Bohm,K., Matsumoto,S., Lingaraju,G.M., Faty,M., Yasuda,T., Cavadini,S., Wakasugi,M.,, Hanaoka,F. *et al.* (2011) The molecular basis of CRL4DDB2/CSA ubiquitin ligase architecture, targeting, and activation. *Cell*, **147**, 1024–1039.
17. Schwechheimer,C. (2004) The COP9 signalosome (CSN): an evolutionary conserved proteolysis regulator in eukaryotic development. *Biochim. Biophys. Acta*, **1695**, 45–54.
18. Wei,N. and Deng,X.W. (2003) The COP9 signalosome. *Annu. Rev. Cell Dev. Biol.*, **19**, 261–286.
19. Kato,J.Y. and Yoneda-Kato,N. (2009) Mammalian COP9 signalosome. *Genes Cells*, **14**, 1209–1225.
20. Menon,S., Tsuge,T., Dohmae,N., Takio,K. and Wei,N. (2008) Association of SAP130/SF3b-3 with Cullin-RING ubiquitin ligase complexes and its regulation by the COP9 signalosome. *BMC Biochem.*, **9**, 1.
21. Moehren,U., Dressel,U., Reeb,C.A., Vaisanen,S., Dunlop,T.W., Carlberg,C. and Baniahmad,A. (2004) The highly conserved region of the co-repressor Sin3A functionally interacts with the co-repressor Alien. *Nucleic Acids Res.*, **32**, 2995–3004.
22. Groisman,R., Polanowska,J., Kuraoka,I., Sawada,J., Saijo,M., Drapkin,R., Kisselev,A.F., Tanaka,K. and Nakatani,Y. (2003) The

ubiquitin ligase activity in the DDB2 and CSA complexes is differentially regulated by the COP9 signalosome in response to DNA damage. *Cell*, **113**, 357–367.

23. Menon,S., Chi,H., Zhang,H., Deng,X.W., Flavell,R.A. and Wei,N. (2007) COP9 signalosome subunit 8 is essential for peripheral T cell homeostasis and antigen receptor-induced entry into the cell cycle from quiescence. *Nat. Immunol.*, **8**, 1236–1245.

24. Ullah,Z., Buckley,M.S., Arnosti,D.N. and Henry,R.W. (2007) Retinoblastoma protein regulation by the COP9 signalosome. *Mol. Biol. Cell*, **18**, 1179–1186.

25. Chamovitz,D.A. (2009) Revisiting the COP9 signalosome as a transcriptional regulator. *Embo. Rep.*, **10**, 352–358.

26. Dessau,M., Halimi,Y., Erez,T., Chomsky-Hecht,O., Chamovitz,D.A. and Hirsch,J.A. (2008) The Arabidopsis COP9 signalosome subunit 7 is a model PCI domain protein with subdomains involved in COP9 signalosome assembly. *Plant Cell*, **20**, 2815–2834.

27. Ellisdon,A.M. and Stewart,M. (2012) Structural biology of the PCI-protein fold. *Bioarchitecture*, **2**, 118–123.

28. Orian,A., Abed,M., Kenyagin-Karsenti,D. and Boico,O. (2009) DamID: a methylation-based chromatin profiling approach. *Methods Mol. Biol.*, **567**, 155–169.

29. Filion,G.J., van Bemmel,J.G., Braunschweig,U., Talhout,W., Kind,J., Ward,L.D., Brugman,W., de Castro,I.J., Kerkhoven,R.M., Bussemaker,H.J. *et al.* (2010) Systematic protein location mapping reveals five principal chromatin types in Drosophila cells. *Cell*, **143**, 212–224.

30. Carey,M.F., Peterson,C.L. and Smale,S.T. (2009) Chromatin immunoprecipitation (ChIP). *Cold Spring Harb. Protoc.*, **2009**, pdb prot5279.

31. Rebhan,M., Chalifa-Caspi,V., Prilusky,J. and Lancet,D. (1997) GeneCards: integrating information about genes, proteins and diseases. *Trends Genet.*, **13**, 163.

32. Heinz,S., Benner,C., Spann,N., Bertolino,E., Lin,Y.C., Laslo,P., Cheng,J.X., Murre,C., Singh,H.,, Glass,C.K. *et al.* (2010) Simple combinations of lineage-determining transcription factors prime cis-regulatory elements requires for macrophage and B cell identities. *Mol. Cell*, **38**, 576–589.

33. Royer,C.A. and Scarlata,S.F. (2008) Fluorescence approaches to quantifying biomolecular interactions. *Methods Enzymol*, **450**, 79–106.

34. Jen-Jacobson,L. (1997) Protein–DNA recognition complexes: conservation of structure and binding energy in the transition state. *Biopolymers*, **44**, 153–180.

35. Roy,S., Ernst,J., Kharchenko,P.V., Kheradpour,P., Negre,N., Eaton,M.L., Landolin,J.M., Bristow,C.A., Ma,L., Lin,M.F. *et al.* (2010) Identification of functional elements and regulatory circuits by Drosophila modENCODE. *Science*, **330**, 1787–1797.

36. Benjamini,Y. and Hochberg,Y. (1995) Controlling the false discovery rate: a practical and powerful approach to multiple testing. *J. Royal Stat. Soc. B*, **57**, 289–300.

37. Smith,S.T., Wickramasinghe,P., Olson,A., Loukinov,D., Lin,L., Deng,J., Xiong,Y., Rux,J., Sachidanandam,R.,, Sun,H. *et al.* (2009) Genome wide ChIP-chip analyses reveal important roles for CTCF in Drosophila genome organization. *Dev. Biol.*, **328**, 518–528.

38. Zhang,H. and Levine,M. (1999) Groucho and dCtBP mediate separate pathways of transcriptional repression in the Drosophila embryo. *Proc. Natl Acad. Sci. U.S.A.*, **96**, 535–540.

39. Acharya,P., Negre,N., Johnston,J., Wei,Y., White,K.P., Henry,R.W. and Arnosti,D.N. (2012) Evidence for autoregulation and cell signaling pathway regulation from genome-wide binding of the Drosophila retinoblastoma protein. *G3*, **2**, 1459–1472.

40. Korenjak,M., Anderssen,E., Ramaswamy,S., Whetstine,J.R. and Dyson,N.J. (2012) RBF binding to both canonical E2F targets and noncanonical targets depends on functional dE2F/dDP complexes. *Mol. Cell. Biol.*, **32**, 4375–4387.

41. Huang,D.W., Sherman,B.T. and Lempicki,R.A. (2009) Systematic and integrative analysis of large gene lists using DAVID bioinformatics resources. *Nat. Protoc.*, **4**, 44–57.

42. Oren-Giladi,P., Krieger,O., Edgar,B.A., Chamovitz,D.A. and Segal,D. (2008) Cop9 signalosome subunit 8 (CSN8) is essential for Drosophila development. *Genes Cells*, **13**, 221–231.

43. Wei,N. and Deng,X.W. (1992) COP9: a new genetic locus involved in light-regulated development and gene expression in Arabidopsis. *Plant Cell*, **4**, 1507–1518.

44. Halimi,Y., Dessau,M., Pollak,S., Ast,T., Erez,T., Livnat-Levanon,N., Karniol,B., Hirsch,J.A. and Chamovitz,D.A. (2011) COP9 signalosome subunit 7 from Arabidopsis interacts with and regulates the small subunit of ribonucleotide reductase (RNR2). *Plant Mol. Biol.*, **77**, 77–89.

45. Fang,L., Kaake,R.M., Patel,V.R., Yang,Y., Baldi,P. and Huang,L. (2012) Mapping the protein interaction network of the human COP9 signalosome complex using a label-free QTAX strategy. *Mol. Cell. Proteomics*, **11**, 138–147.

46. Fang,L., Wang,X., Yamoah,K., Chen,P.L., Pan,Z.Q. and Huang,L. (2008) Characterization of the human COP9 signalosome complex using affinity purification and mass spectrometry. *J. Proteome Res.*, **7**, 4914–4925.

47. Olma,M.H., Roy,M., Le Bihan,T., Sumara,I., Maerki,S., Larsen,B., Quadroni,M., Peter,M., Tyers,M. and Pintard,L. (2009) An interaction network of the mammalian COP9 signalosome identifies Dda1 as a core subunit of multiple Cul4-based E3 ligases. *J. Cell. Sci.*, **122**, 1035–1044.

48. Chamovitz,D.A. and Segal,D. (2001) JAB1/CSN5 and the COP9 signalosome. A complex situation. *EMBO. Rep.*, **2**, 96–101.

49. Sikder,D., Johnston,S.A. and Kodadek,T. (2006) Widespread, but non-identical, association of proteasomal 19 and 20 S proteins with yeast chromatin. *J. Biol. Chem.*, **281**, 27346–27355.

50. Abed,M., Barry,K.C., Kenyagin,D., Koltun,B., Phippen,T.M., Delrow,J.J., Parkhurst,S.M. and Orian,A. (2011) Degringolade, a SUMO-targeted ubiquitin ligase, inhibits Hairy/Groucho-mediated repression. *EMBO J.*, **30**, 1289–1301.

51. Kwon,J.E., La,M., Oh,K.H., Oh,Y.M., Kim,G.R., Seol,J.H., Baek,S.H., Chiba,T., Tanaka,K., Bang,O.S. *et al.* (2006) BTB domain-containing speckle-type POZ protein (SPOP) serves as an adaptor of Daxx for ubiquitination by Cul3-based ubiquitin ligase. *J. Biol. Chem.*, **281**, 12664–12672.

52. Braun,S. and Madhani,H.D. (2012) Shaping the landscape: mechanistic consequences of ubiquitin modification of chromatin. *EMBO Rep.*, **13**, 619–630.